Stem Cell Research 23 (2017) 1–12

Contents lists available at ScienceDirect

Stem Cell Research

journal homepage: www.elsevier.com/locate/scr

Isolation and functional interrogation of adult human prostate epithelial stem cells at single cell resolution

Wen-Yang Hu [a], Dan-Ping Hu [a], Lishi Xie [a], Ye Li [a], Shyama Majumdar [a], Larisa Nonn [b,c], Hong Hu [d], Toshi Shioda [e], Gail S. Prins [a,b,c,*]

[a] Department of Urology, College of Medicine, University of Illinois at Chicago, Chicago, IL 60612, USA
[b] Department of Pathology, College of Medicine, University of Illinois at Chicago, Chicago, IL 60612, USA
[c] University of Illinois Cancer Center, College of Medicine, University of Illinois at Chicago, Chicago, IL 60612, USA
[d] Research Resources Center, University of Illinois at Chicago, Chicago, IL 60612, USA
[e] Massachusetts General Hospital Center for Cancer Research and Harvard Medical School, Charlestown, MA 02129, USA

ARTICLE INFO

Article history:
Received 27 March 2017
Received in revised form 19 May 2017
Accepted 14 June 2017
Available online 16 June 2017

Keywords:
Prostate
Stem cell
Progenitor cell
Prostasphere
Prostate cancer

ABSTRACT

Using primary cultures of normal human prostate epithelial cells, we developed a novel prostasphere-based, label-retention assay that permits identification and isolation of stem cells at a single cell level. Their *bona fide* stem cell nature was corroborated using *in vitro* and *in vivo* regenerative assays and documentation of symmetric/asymmetric division. Robust WNT10B and KRT13 levels without E-cadherin or KRT14 staining distinguished individual stem cells from daughter progenitors in spheroids. Following FACS to isolate label-retaining stem cells from label-free progenitors, RNA-seq identified unique gene signatures for the separate populations which may serve as useful biomarkers. Knockdown of *KRT13* or *PRAC1* reduced sphere formation and symmetric self-renewal highlighting their role in stem cell maintenance. Pathways analysis identified ribosome biogenesis and membrane estrogen-receptor signaling enriched in stem cells with NF-κB signaling enriched in progenitors; activities that were biologically confirmed. Further, bioassays identified heightened autophagy flux and reduced metabolism in stem cells relative to progenitors. These approaches similarly identified stem-like cells from prostate cancer specimens and prostate, breast and colon cancer cell lines suggesting wide applicability. Together, the present studies isolate and identify unique characteristics of normal human prostate stem cells and uncover processes that maintain stem cell homeostasis in the prostate gland.

1. Introduction

The adult prostate gland contains a simple columnar epithelium composed of luminal secretory and underlying basal cells with a scarce neuroendocrine cell component. These epithelial cells are derived from a rare, relatively quiescent stem cell population that maintains glandular homeostasis throughout life (Leong et al., 2008). While prostate epithelial stem cells and their progeny have been investigated in rodent models and humans, their unique characteristics and lineage hierarchy remain a topic of debate. Credible evidence suggests that there may be a common precursor stem cell for all lineages while other findings support distinct basal and luminal stem cell populations within the adult prostate. These two scenarios are not mutually exclusive as emerging data indicates inherent plasticity and stage/context-specific utilization of stem and progenitor cell populations. In rodent models, prostate homeostasis appears to be maintained by both luminal and basal unipotent progenitor cells as well as bipotent stem/progenitor cells that exist in both compartments (Ousset et al., 2012; Toivanen et al., 2016; Wang et al., 2015; Wang et al., 2013; Xin et al., 2007). Although stem cell traits and lineage hierarchy for the human prostate epithelium are less studied, lineage tracing techniques using mitochondrial mutations have clearly demonstrated that basal, luminal and neuroendocrine cell lineages in the adult prostate are derived from a common precursor stem cell (Blackwood et al., 2011; Gaisa et al., 2011). Most current evidence from human prostate tissues suggests that normal stem cells primarily reside within the basal cell compartment (Goldstein et al., 2008; Zhang et al., 2016).

Advances in prostate cancer research have identified resident cancer stem-like cells that are intrinsically resistant to standard treatments and reseed tumor growth following ablative therapies (Chen et al., 2016; Collins et al., 2005; Yun et al., 2016). Furthermore, gene profiling analysis has shown that prostate cancer increases in a stem-like state as it progresses from organ-confined to metastatic disease (Smith et al., 2015). Consequently, it is imperative to develop therapeutic modalities that target the prostate cancer stem-like population for effective disease management. Although prostate cancer stem cells will be distinct from

* Corresponding author at: Department of Urology, University of Illinois at Chicago, 820 South Wood St., M/C 955, Chicago, IL, 60612, USA
E-mail address: gprins@uic.edu (G.S. Prins).

http://dx.doi.org/10.1016/j.scr.2017.06.009

normal prostate stem cells (Chen et al., 2016), similarities could be capitalized on for therapeutic advantage. Thus a fundamental understanding of normal human prostate stem cell properties and the factors that modulate their self-renewal and lineage commitment may provide new insights into the origin and treatment of prostate cancer.

Approaches for isolating prostate stem cells have primarily utilized flow cytometry and 3D spheroid culture (Hu et al., 2011; Leong et al., 2008; Xin et al., 2007). However, a detailed characterization has been hindered by their lack of specificity and selectivity. Utilization of FACS with different antibodies against multiple surface antigens have yielded variable results (Collins et al., 2005; Vander Griend et al., 2008; Williamson et al., 2013), raising questions on the identity of the isolated cells. While resident stem cells are typically growth quiescent *in vivo*, when placed in 3D matrix culture without niche restraints, they undergo asymmetric division, generating progenitor cells that rapidly proliferate and lineage commit. Whereas the prostasphere (PS) culture system has been useful to enrich stem and progenitor cell populations, the resulting spheroids are a heterogeneous mixture of these cells types (Fig. 1C), making the identification of unique stem cell properties inconclusive. Clearly, improved assays to recognize and separate prostate stem cells are essential to move the field forward. Towards that end, the overall goal of the present study was to develop a system that permits clear identification and isolation of purified stem cells from human prostate specimens and conduct robust downstream analysis of their functional properties.

The approach for stem cell identification utilized herein is functional, based on the relative quiescence and thus label retention property of stem cells within a mixed epithelial population. Long-term 5-bromo-2′-deoxyuridine (BrdU) retention has been previously used to label stem cells *in vivo* and *in vitro* based on their prolonged doubling time (Cicalese et al., 2009; Klein and Simons, 2011). In addition, the immortal strand DNA hypothesis suggests that as stem cells undergo asymmetric division, the older parental DNA segregates into one daughter stem cell while the other daughter cell receives newly synthesized DNA and becomes a committed progenitor cell (Cairns, 1975). This unique situation allows the opportunity to BrdU-label DNA in parental stem cells within primary cultures and monitors their properties following BrdU-washout upon transfer to 3D spheroid culture. In the present studies, this pulse-chase approach was applied to primary prostate epithelial cultures derived from healthy organ donors, as opposed to benign regions from patient specimens, to ensure lack of a modifying disease field effect. While primary prostate epithelial cells adapt a basal and transit amplifying phenotype in 2D culture, they also contain the rare multipotent stem cells as evidenced by formation of fully differentiated organoids or differentiated spheroids upon transfer to 3D systems (Hu et al., 2011; Karthaus et al., 2014). By using PS-based BrdU/CFSE/Far red retention assays followed by FACS sorting, we herein identify label-retaining spheroid cells at a single cell resolution. Importantly, they exhibit stem cell characteristics including asymmetric cell division with segregation of parental DNA in daughter stem cells, *in vitro* serial

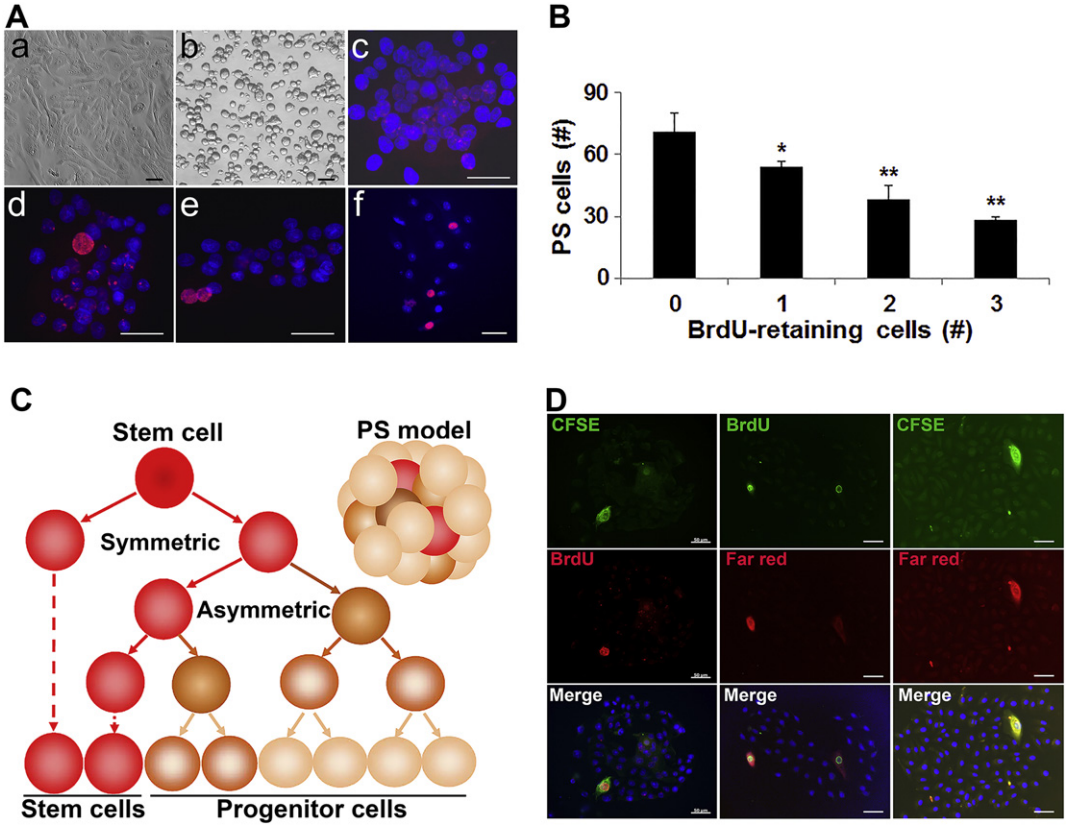

Fig. 1. Prostate stem cell identification by prostasphere-based label-retention assay. (A): 2D primary PrEC (a) were BrdU labeled and transferred to 3D culture with PS harvested on day 5 (b). BrdU immunostaining (pink) identified stem-like cells with retention of parental DNA (c-f). Any BrdU label in rapidly dividing progenitor cells (DAPI, blue) was diluted and lost (c-f). Representative images of whole PS with different numbers of BrdU$^+$ label-retaining cells (0-c, 1-d, 2-e, 3-f). (B): Graph shows an inverse relationship between BrdU$^+$ cells and PS cell number. *P < 0.05, **P < 0.01 *vs* zero BrdU$^+$ cell group. N = 12, 33, 29 and 12 for spheres with 0, 1, 2 and 3 BrdU$^+$ cells, respectively. (C): Proposed model for stem cell hierarchy as a PS is formed. In response to the stem cell niche, quiescent prostate stem cells (solid red) undergo symmetric self-renewal or asymmetric cell division. Symmetric self-renewal yields two daughter stem cells that can remain quiescent (left) or undergo asymmetric division (right). Asymmetric division generates one daughter stem cell (red) and one early stage progenitor cell (dark brown). As progenitor cells divide and lineage commit, they give rise to middle (partial brown) and late (light brown) stage progenitor cells. (D): Fluorescent pro-dyes CFSE and Far-red exclusively label BrdU-retenting PS cells. PrEC cells labeled with BrdU were treated with CFSE or Far-red and transferred to label-free PS culture. Day 5 PS stained for BrdU plus CFSE (green) or Far-red (red) showed signal co-localization upon fluorescence imaging. Representative images show BrdU/CFSE (left panel), BrdU/Far-red (middle panel) and CFSE/Far-red (right panel) co-labeling in a single PS cell. Scale bars = 50 μm.

passage and *in vivo* prostate regenerative capacity, augmented autophagy flux, increased ribosome biogenesis and reduced metabolic activity relative to the lineage committed progenitor cells within early-stage spheroids. RNA-seq revealed differentially expressed genes in the stem-like cells including cytokeratin 13 (*KRT13*) and prostate cancer susceptibility candidate 1 (*PRAC1*) that may serve as novel biomarkers for human prostate stem cells. Application of this approach to cancer specimens and cell lines identified a small number of label-retaining cancer stem-like cells which may provide translational opportunities to target this therapeutic resistant population.

2. Materials and methods

2.1. Cell and PS cultures

Primary human prostate epithelial cells (PrEC) were obtained from four young (19–21 yrs) disease-free organ donors (Lifeline Cell Technology, Frederick, MD) and cultured in ProstaLife Epithelial Cell Growth Medium (PrEGM) as described (Hu et al., 2011; Prins et al., 2014). PrE-Ca were isolated from radical prostatectomy tissue at the UIC Hospital with Institutional Review Board approval. DU145, MCF-7 and HCT116 cancer cell lines were obtained from ATCC. PS were cultured from primary PrEC using a previously described serum-free 3D Matrigel (Corning) system and confirmed as clonally-derived spheroids of stem/progenitor cells (Hu et al., 2011). See Supplementary material for further culture details.

2.2. Spheroid-based BrdU and CFSE/far-red label-retention assay

Parental PrEC or cancer cells were 2D cultured with 1 μM BrdU (Sigma-Aldrich) for 10 days for labeling of dividing cells. Cells were transferred to 3D Matrigel culture for 5 days to permit BrdU wash-out during spheroid growth (~6 cell cycles). PS were harvested by dispase digestion and attached to chamber slides during overnight culture in PrEGM. Spheres were fixed in ice cold acetone/methanol (1:1) and immunostained using mouse anti-BrdU antibody.

For CFSE/Far-red label-retention of live cells, parental PrEC were 2D cultured ± 1 μM BrdU for 10 days followed by 5 μM CFSE (5(6)-Carboxyfluorescein *N*-hydroxysuccinimidyl ester) or Far-red (Life Technologies, Grand Island, NY) labeling for 30 min. Labeled PrEC were plated in 3D Matrigel in the absence of labels and PS cultured for 5 days. PSs were harvested as above and immunofluorescent stained for BrdU. Co-labeled $BrdU^{+}$ and CFSE/Far-red label-retaining cells were identified and imaged by fluorescent microscopy (Zeiss Axioskop).

2.3. Immunocytochemistry

See Supplementary material.

2.4. Live cell separation by fluorescence-activated cell sorting

Analysis of trypsin-dispersed CFSE-labeled PS cells was performed by single-channel FACS (CyAn™ ADP Analyzer, Beckman Coulter Inc., Brea, CA) using the Summit Software polygon tool. Subpopulations of fractionated $CFSE^{Hi}$, $CFSE^{Med}$ and $CFSE^{Lo}$ cells were gated based on the negative and positive controls using the FACS-DiVa software polygon tool and collected by CellSorter (MoFlo™XDP, Beckman).

2.5. PS-based paired cell, limiting dilution and clonal assays

For paired-cell analysis, BrdU-labeled PS were cultured to day 5, trypsin-dispersed into single cells, plated on chamber slides and cultured overnight in PrEGM to permit one cell division. Cells were fixed and immunostained for BrdU. Images of paired cells (distance between two nuclei <30 μm) were taken with a Zeiss Axioskop20 fluorescence microscope and, based on BrdU-segregation, were classified as stem cell symmetric or asymmetric division.

For clonal analysis, single live CFSE-retaining cells were sorted into 96-well plates (1 cell/well) and 3D cultured in Matrigel. PS formation from a single cell was evaluated at day 10 and sphere-forming efficiency was calculated. For limiting-dilution analysis, live CFSE-retaining single cells were sorted into 96-well plates with 10, 25, 50 or 100 cells/well for 3D spheroid culture. PS formation was evaluated at day 10 and absence of sphere formation over a range of cell numbers was used to calculate the minimum number of cells required for PS growth.

2.6. Tissue recombination and renal grafts

See Supplementary material.

2.7. Autophagy analysis

See Supplementary material.

2.8. Next generation RNA-sequencing analysis

Transcriptomal profiles of $CFSE^{Hi}$ and $CFSE^{Lo}$ cells were determined by RNA-seq (Miyamoto et al., 2015). Following cDNA synthesis and fragmentation, indexed deep sequencing libraries for Illumina NextSeq 500 sequencing were generated and library quantitations and size distributions were determined using Agilent Tapestation. Paired-end sequencing (75 nt + 75 nt) yielded >50 million raw reads, which were aligned to the human GRCh38 reference genome sequence. See Supplementary material for further details and bioinformatics analysis.

2.9. RT-PCR

See Supplementary material.

2.10. Seahorse mitochondrial-stress assay

See Supplementary material.

2.11. Statistical analysis

All experiments were biologically replicated 3–6 times. Data were analyzed using Students' *t*-test or for multiple groups, ANOVA followed by Student-Newman-Keuls test. Values are expressed as means ± SEM, and a value of $P < 0.05$ was considered significant.

3. Results

3.1. Identification of long-term label-retaining cells in primary Prostaspheres

Primary human prostate epithelial cells (PrEC) from young disease-free organ donors were used to enrich and expand prostate stem and daughter progenitor cells using a PS assay. As previously characterized (Hu et al., 2011), ~0.1–0.5% of PrEC with stem-like characteristics survive and form clonally-derived PS when transferred to a 3D Matrigel culture system whereas differentiated PrEC fail to survive (Fig.1Aa-b). To identify and isolate the rare prostate stem-like cells within the spheroid, parental PrEC cells were BrdU-labeled for 10 days in 2D culture to maximize labeling of the infrequently dividing stem cell population. A wash-out phase commenced upon transfer to 3D Matrigel culture and at day 5, the early-stage PS were fixed and immunostained with BrdU-antibody. The relatively quiescent stem cells within each sphere retained most of the parental DNA, visualized by strong $BrdU^{+}$ staining and identified at the single cell level (Fig.1Ad–f; Supplemental Video 1). In contrast, any BrdU-labeled DNA remaining in rapidly dividing daughter progenitors was quickly diluted resulting in weakly positive or

negative BrdU stain (Fig.1Ac–f). The majority of PS (>80%) contained 1–3 $BrdU^+$ stem-like cells/sphere while a smaller fraction had no visible strong $BrdU^+$ cell (Fig.1Ac). These later spheroids are postulated to arise from a stem cell that did not divide during the BrdU pulse. PS size was inversely related to the $BrdU^+$ cell number with BrdU-negative spheres containing ~70 cells whereas those with 2–3 $BrdU^+$ cells contained ~25–40 cells on day 5 (Fig.1B). The slower PS growth with more $BrdU^+$ cells likely results from the sphere-initiating stem cell first undergoing symmetric self-renewal, giving rise to 2 $BrdU^+$ stem-like cells, prior to asymmetric division to generate daughter progenitor cells, thus delaying entry into the rapid amplification phase of progenitor proliferation (see model, Fig. 1C).

To enable identification and isolation of live stem-like cells from spheroids, pro-dyes were substituted for BrdU. CFSE (5(6)-Carboxyfluorescein N-hydroxysuccinimidyl ester) is a cell permeable, non-fluorescent pro-dye. Upon entry into live cells, intracellular esterases cleave CFSE acetate groups and produce carboxyfluorescein, a membrane impermeable green fluorescent dye that is diluted only upon cell division. Day 5 PS co-labeled with BrdU and CFSE revealed that a strong CFSE signal was retained exclusively in $BrdU^+$ cells (Fig. 1D). Similarly, co-labeling PrEC cells with the fluorescent pro-dye Far Red and either BrdU or CFSE prior to 5 days of 3D culture revealed exclusive staining of all markers within a rare PS cell population (Fig. 1D). Together these results provide strong support that the BrdU/CFSE/Far red retention assay labels a scarce PS cell type that is relatively quiescent and may represent the prostate epithelial stem cell that initiates spheroid growth.

3.2. Label-retaining PS cells exhibit stem cell properties

Live cell FACS was utilized to capture the long-term label-retaining cells for subsequent characterization. Day 5 CFSE-labeled PS were dispersed to single cells and sorted for $CFSE^+$ signal with ~1.0% of sphere cells gated as $CFSE^{Hi}$, ~2–3% as $CFSE^{Med}$ signal and ~95–97% of PS cells as $CFSE^{Lo}$ across multiple runs (Fig. 2A). Imaging of $CFSE^{Hi}$ and $CFSE^{Lo}$ cell fractions confirmed the clean separation of $CFSE^+$ and $CFSE^-$ cells (Fig. 2B) and revealed the larger size of $CFSE^+$ cells relative to $CFSE^-$ cells. Since spheroid serial passage is a measure of stemness, the sorted $CFSE^{Hi}$, $CFSE^{Med}$ and $CFSE^{Lo}$ PS cells were replated in 3D cultures. While $CFSE^{Hi}$ cells retained robust sphere-forming capability, this was limited in $CFSE^{Med}$ cells and lost completely in $CFSE^{Lo}$ cells (Fig.2Ca–c, D) indicating that only $CFSE^{Hi}$ cells have stem cell properties. Further, single $CFSE^{Hi}$ sorted cells could form a single PS in clonal 3D culture (Fig. 2Cd–f), but not single $CFSE^{Med}$ or $CFSE^{Lo}$ cells. A limited dilution assay demonstrated that PS forming efficiency increased with increasing numbers of $CFSE^{Hi}$ cells in culture (Fig.2E). Next, the prostate regenerative ability of $CFSE^{Hi}$ cells was evaluated *in vivo*. When mixed with rat embryonic urogenital sinus mesenchyme (UGM) and renal grafted *in vivo*, $CFSE^{Hi}$ cells generated prostate-like tissues (Fig. 2Fa,c) at a graft rate of 50% whereas $CFSE^{Lo}$ cells had no tissue-forming capacity (Fig. 2F–G). PSA^+ staining of the graft tissue demonstrated the human origin and full epithelial differentiation (Fig. 2Fd). Together, these *in vitro* and *in vivo* data indicate that long-term label-retaining PS cells represent the prostate epithelial stem cells whereas the $BrdU^-/CFSE^-$ cells, which constitute the bulk of the PS, are committed progenitor cells.

3.3. Analysis of symmetric and asymmetric cell division in label-retaining stem cells

One hallmark property of stem cells is their ability to undergo symmetric and asymmetric cell divisions (Neumuller and Knoblich, 2009; Wang et al., 2014). To assess these division types, day 5 PS were dispersed to single cells, cultured overnight and stained for CD49f, a high-expressed integrin in prostate stem cells. Three cell division types were detected (Fig. 3A): 1) $CD49f^{Hi}$ stem cell symmetric self-renewal; 2) asymmetric division with one $CD49f^{Hi}$ and one $CD49f^{Lo}$ daughter cell; and 3) $CD49f^{Lo}$ symmetric division of progenitor cells. To confirm and quantitate symmetric and asymmetric cell divisions in $BrdU^+$ label-retaining cells, a paired-cell assay was performed (Fig. 3B). Upon stem cell symmetric self-renewal, parental DNA was evenly distributed into two daughter stem cells ($BrdU^{+/+}$). During asymmetric division, the $BrdU^+$ labeled parental DNA segregated into one daughter cell while the other received newly synthesized, largely $BrdU^-$ DNA ($BrdU^{+/-}$). Quantitation of these division types revealed that symmetric self-renewal was a rare event with 3.1% frequency while asymmetric cell division constituted 96.9% of stem cell divisions.

3.4. Label-retaining stem cells exhibit low cytokeratin 14 (KRT 14) and E-cadherin and elevated WNT10B

$BrdU^+$ label-retaining cells were examined for expression of known prostate epithelial cell markers. The paired-cell assay for asymmetric division revealed a striking pattern of basal cell KRT14 with $BrdU^+$ stem cells as $KRT14^-$ and daughter progenitor cells as strongly $KRT14^+$ (Fig. 3Ca). Similar patterns were noted in the intact PS (Figs. 3C-b, S1A). Further, while PS progenitor cells strongly expressed E-cadherin, the $BrdU^+/CFSE^+$ cells were consistently E-cadherin negative (Figs. 3Cc, S1A). WNT10B, required for stem cell differentiation into prostate organoids (Calderon-Gierszal and Prins, 2015), was selectively localized to $BrdU^+$ labeled cells with limited staining in daughter progenitor cells (Figs. 3C-d, S1A). Of note, long-term label-retaining stem cells remained uniquely separated from the PS non-labeled cells as shown in $CFSE^{Hi}$ (Fig. 3D arrow, F). Further, these label-retaining stem cells had larger nuclear diameter and area relative to the non-labeled cells (Fig. 3E). The larger nuclei may be a function of relative quiescence in stem cells whereas the isolation pattern may reflect limited cell adhesion/junction proteins such as E-cadherin. Together, these data support an uncommitted stemness state of label-retaining cells.

3.5. Label-retaining stem cells possess augmented autophagy activity

Increased autophagy has been shown in therapy-resistant cancer cells and enhances survival in long lived stem cells (Guan et al., 2013). Herein, the $BrdU^+$ PS cells exhibited increased LC3 protein particles implicating augmented autophagosome formation (Fig.3G, S1A). To assess activity, autophagy flux was monitored in label-retaining cells using an mCherry-GFP-LC3 expression vector (Figs. 3H, S1B). Far-red^+ label-retaining cells specifically showed high LC3-mCherry staining (pH insensitive) with loss of GFP label (pH-sensitive) indicating fusion of autophagosomes with acidic lysosomes. This marks the stem cell as having robust autophagy flux. In contrast, the progenitor cells exhibited weaker LC3-mCherry labeling and retention of GFP indicating limited autophagic flux.

3.6. RNA-Seq identifies the enriched pathways and transcriptome profiles of prostate stem and progenitor cell populations

$CFSE^{Hi}$ and $CFSE^{Lo}$ cell populations isolated by FACS from 2 to 3 biologic replicates, respectively, were subjected to transcriptomal profiling by RNA-seq to obtain insights into biological characteristics of stem and progenitor cells. Gene set enrichment analysis (GSEA) detected 3 significantly enriched pathways/processes (FDR $q < 0.05$, FWER $P < 0.05$). First, the $CFSE^{Hi}$ stem cells were markedly enriched for ribosome/translational regulation processes associated with 88 ribosome protein genes relative to $CFSE^{Lo}$ cells (Figs. 4A, S2A–B). Ribosome biogenesis initiates in the nucleolus. Accordingly, FACS sorted $CFSE^{Hi}$ cells and $BrdU^+$ cells in whole PS bore prominent and larger nucleoli with robust levels of Nucleolin protein relative to $CFSE^{Lo}$ cells (Fig. 4B), supporting enhanced ribosome biogenesis in stem cells. The second GSEA pathway identified enrichment of plasma membrane estrogen receptor (ER) signaling associated with 40 genes in $CFSE^{Hi}$ cells (Figs. 4A, S2C). Our laboratory recently identified robust ER activity in PS cells with ERβ enrichment in $BrdU^+$ retaining cells and ERα enrichment in progenitor cells (Hu et

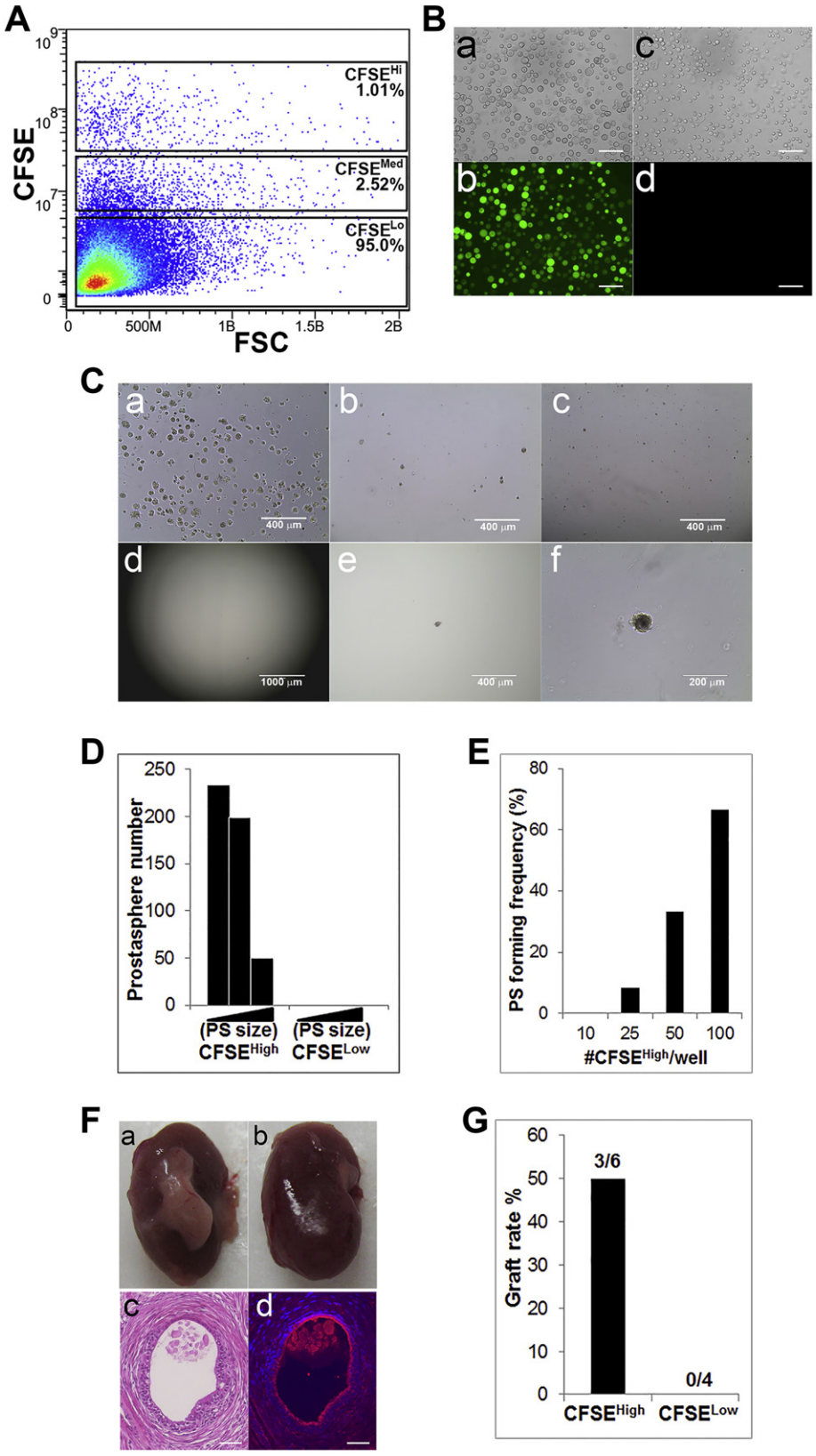

Fig. 2. CFSE^{Hi} label-retaining cells exhibit stem cell self-renew and regenerative properties. (A): Cell isolation by FACS. Day 5 CFSE-labeled PSs were dispersed to single cells and sorted for CFSE-label. CFSE-retaining cells (CFSE^{Hi}, 1.01%) and non-retaining cells (CFSE^{Med} 2.52%; CFSE^{Lo} 95.0%) were gated and collected by live cell sorting. (B): Representative bright field (a,c) and fluorescent (b,d) images of CFSE^{Hi} (a-b) and CFSE^{Lo} cells (c-d) with CFSE in green. (C): a-c; CFSE^{Hi} cells show significantly higher PS forming ability than CFSE^{Med} and CFSE^{Lo} cells. Representative images of PS formation from sorted CFSE^{Hi} (a), CFSE^{Med} (b) and CFSE^{Lo} (c) cells. d-f; Single cell sorting followed by clonal culture assay shows a single CFSE^{High} cell formed one PS. Images show culture on day 1 (d), day 3 (e) and day 10 (f). Scale bars = 50 μm. (D): Histogram shows number PS formed from CFSE^{Hi} and CFSE^{Lo} cells across 3 size categories (40–60, 60–80, and >80 μM diameter) at second passage. (E): Limited dilution assay of CFSE^{Hi} cells (10, 25, 50, 100 cells/well) shows PS forming efficiency correlates with cell number. (F): CFSE^{Hi} (a) but not CFSE^{Lo} cells (b) formed glandular prostate-like tissues (c) when renal grafted with rat UGM. (d) PSA immunostain of grafted tissue (red). Scale bars = 200 μm. (G): *In vivo* graft rate of CFSE^{Hi} (50%) *vs* CFSE^{Lo} cells (0%) using ~1000 cells/graft.

al., 2011; Prins et al., 2015). Notably, estrogen exposure enhances stem cell symmetric self-renewal and progenitor cell amplification, effects mediated in part through membrane-initiated ER signaling that includes MAPK/ERK and PI3K/AKT activation (Prins et al., 2014), together providing biologic support for GSEA enrichment of this pathway. Finally, GSEA identified NF-κB pathway enrichment for 23 genes in $CFSE^{Lo}$ progenitor cells (Figs. 4A, S2D). Prostate cancer stem-like and progenitor cells were previously shown as NF-κB enriched relative to committed epithelial cells using gene expression array analysis (Birnie et al., 2008). Further, the NF-κB family of transcription factors is required for normal neural progenitor cell proliferation using TNFα signaling through TNFR2 (Chen and Palmer, 2013), both enriched in the $CFSE^{Lo}$ cells. To test the role of NF-κB signaling in progenitor cell proliferation directly, PS were cultured with IKK VII, an inhibitor of TNFα-stimulated IκB degradation. PS size, a marker of progenitor cell proliferation, was significantly reduced after 7 days (Fig. 4C). Further, an accumulation of cyclin E and loss of cyclin A expression in IKK VII-exposed spheroids (Fig. 4D), indicates an NF-κB pathway requirement for G1 to S cell cycle transition in prostate progenitor cells.

Next, differential analysis of RNA-seq data identified 203 significant differentially expressed genes (DEGs) between the $CFSE^{Hi}$ and $CFSE^{Lo}$ cell populations (FDR < 0.1) (Fig. 5A). The $CFSE^{Hi}$ stem cells were significantly enriched for 91 genes relative to progenitors whereas the $CFSE^{Lo}$ progenitor cells were preferentially enriched for 112 genes (Tables S1, S2). The DEGs with the highest fold-change in stem cells include *SLC29A4*, *KRT13*, cut-like homeobox 2 (*CUX2*), leukemia inhibitory factor receptor (*LIF-R*) and insulin-like growth factor 2 (*IGF2*) whereas prominent DEGs in progenitor cells include *MAP3K14*, prostaglandins E synthase (*PTGS*), mesothelin (*MSLN*) and LIM homeobox 1 (*LHX1*). The transcriptome was next queried for known stemness and differentiation genes (Fig. 5B). $CFSE^{Hi}$ cells were enriched for multiple stemness genes including Nestin, *SOX2*, Nanog, *LIF-R* and aldehydrogenase1A2 (*ALDH1A2*) whereas $CFSE^{Lo}$ cells exhibited up-regulation of differentiation genes including *KRT*s 5, 8, 18 and 19, androgen receptor (*AR*), carbonic anhydrase IX (*CA9*), Inhibitor of Differentiation 4 (*ID4*) and epidermal growth factor (*EGF*), further confirming their identity as stem and progenitor populations, respectively.

3.7. $CFSE^{High}$ stem cells exhibit decreased mitochondrial metabolism

To gain biologic insight into gene networks and pathways that may regulate stemness and binary cell fate decisions, gene ontology using DAVID pathway enrichment analyses was run on the 203 DEGs ($P < 0.05$). Several processes were enriched in this gene set with metabolic process genes as the top pathway, having 112 down-regulated genes in $CFSE^{Hi}$ cells relative to $CFSE^{Lo}$ progenitors (Fig. 5C, D). We next examined cellular metabolism using the Seahorse Bioscience mitochondria-stress assay. As compared to $CFSE^{Lo}$ cells, mitochondrial respiration in $CFSE^{Hi}$ stem cells was significantly lower for both basal and maximal oxygen consumption rates (Fig. 5E). Further, $CFSE^{Hi}$ cells exhibited overall lower basal extracellular acidification rates, a measure of basal glycolosis, relative to $CFSE^{Lo}$ cells (Fig. 5F). Together, these findings identify lower anabolic metabolism in prostate stem cells compared to daughter progenitors which reflects or contributes to their differential proliferative activities.

3.8. Knockdown of KRT13 or PRAC1 inhibits stem cell self-renewal

Two genes with significantly elevated expression in the $CFSE^{Hi}$ cells were further studied for their role in stem cell maintenance. KRT13 was a top-ranked DEG with 78.2-fold increased levels in the $CFSE^{Hi}$ cells relative to $CFSE^{Lo}$ cells. Using immunofluorescence, KRT13 was specifically localized to the $BrdU^{+}$ retaining cells while daughter progenitor cells were KRT13 low (Figs. 6A, S1A). This pattern was opposite of KRT14 localization, suggesting that KRT13 may be a critical intermediate filament of the prostate stem cell. To test this directly, we knocked-down *KRT13* in PrEC cells using siRNA and, upon transfer to 3D culture, observed a significant reduction in PS formation and number of $BrdU^{+}$ retaining cells/PS (Fig. 6B–E). Another gene of interest was prostate cancer susceptibility candidate1 (*PRAC1*), expressed at 4.2-fold higher levels in $CFSE^{Hi}$ cells. *PRAC1* knockdown using siRNA severely reduced spheroid formation and decreased $BrdU^{+}$ retaining cells/PS by 50% (Fig. 6F-I). Together, these results suggest that KRT13 and PRAC1 play essential roles in maintaining stem cell homeostasis and symmetric self-renewal.

3.9. Identification of cancer stem-like cells using sphere-based label-retaining assay

To test whether long-term $BrdU^{+}/CFSE^{Hi}$ labeling can be used to identify stem-like cells in prostate cancer, we performed PS-based $BrdU^{+}$ retention assays using primary cultures of prostate cancer cells (PrE-Ca) and the prostate cancer cell line DU145. Spheroids grown from both contained a small number of long-term $BrdU^{+}$ retaining cells that exhibited selectively reduced E-cadherin, elevated LC3 and strong KRT13 staining relative to daughter progenitors suggesting similar characteristics of cancer stem-like cells to normal stem cells (Fig. 7A–B). Further, three division types were observed in the cancer stem-like $BrdU^{+}$ retaining cells using the paired cell assay, representing stem cell symmetric self-renewal, asymmetric cell division and committed progenitor cell division (Fig. 7C–D). CFSE-labeling combined with FACS readily isolated the cancer stem-like cells from both PrE-Ca and DU145 spheroids, constituting ~1% of cells (Fig. 7E–F). Similarly, breast cancer (MCF-7) and colon cancer (HCT116) cell lines pre-labeled with BrdU/CFSE in 2D culture formed mammospheres and colonospheres in 3D culture with lone $BrdU^{+}$ label-retaining cells (Fig. 7A). Together, this suggests that the present approaches have broad versatility for identifying and isolating cancer stem-like cells in many epithelial cancer cell types.

4. Discussion

The present study utilized a long-term label-retaining approach to identify, isolate and characterize adult human prostate stem cells from young disease-free organ donors. Detailed analyses confirm the *bona fide* stem cell nature of these isolated cells using *in vitro* and *in vivo* assays of regenerative capability, unique gene expression profiles and the documentation of symmetric/asymmetric cell division, classic indicators of stemness. By use of this biologic-based approach, we identify several novel properties of prostate stem cells hitherto unknown or underappreciated. These include heightened autophagy flux and asymmetric DNA inheritance to maintain stem cell integrity, decreased mitochondrial metabolism, heightened ribosome biogenesis and elevated expression of specific genes that may be useful as prostate stem cell markers in tissue and cultured cell populations. That this approach can similarly be utilized for identifying cancer stem-like cells from primary specimens and cell lines provides an avenue for detailed interrogation of this elusive cancer cell population.

Several novel markers for normal prostate stem cells were identified in the present studies. E-cadherin, a cell adhesion-junction protein, is an epithelial differentiation marker that is down-regulated in stem-like cells and cancer cells undergoing EMT (Graff et al., 1995; Toivanen et al., 2016). Herein, we find E-cadherin is absent in normal prostate stem cells but robust within daughter progenitors. Since RNA-seq data found comparable E-cadherin mRNA in the cell types, the limited protein in stem cells may reflect increased endocytosis or protein degradation (Bryant and Stow, 2004). *Wnt10b* is an early and specific marker of prostate epithelial buds during murine embryogenesis (Allgeier et al., 2010) and is essential for directed differentiation of hESC into prostate organoids (Calderon-Gierszal and Prins, 2015). The present data is the first to identify the selective expression of canonical WNT10B in prostate stem cells. As Wnt signaling is known to play a crucial role in

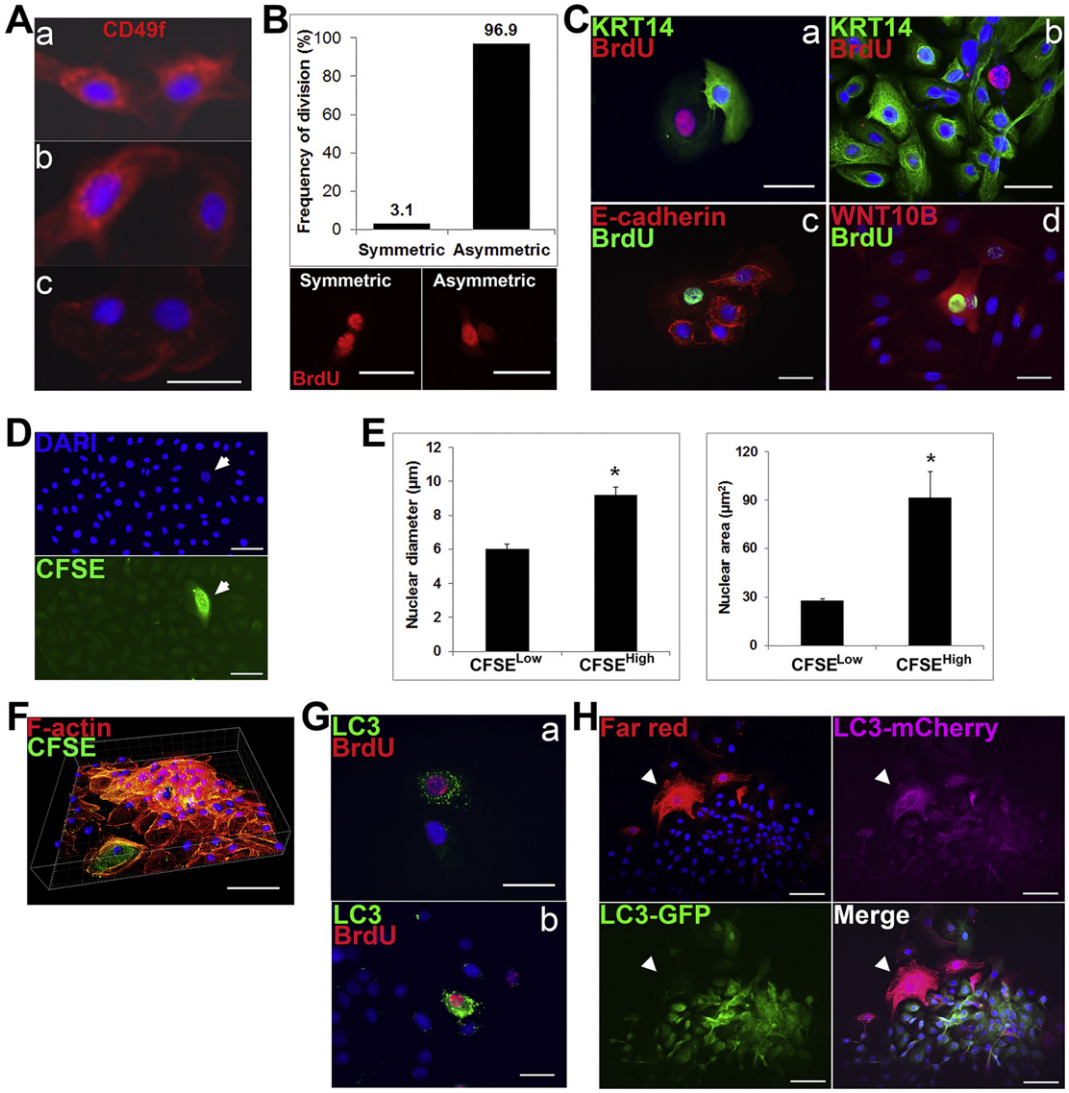

Fig. 3. Label-retaining cells exhibit stem cell characteristics including symmetric and asymmetric stem cell division, a KRT14$^-$/E-cadherin$^-$/WNT10B$^+$ signature, distinct morphology, and increased autophagy flux. (A): Paired-cell analysis of dividing PS cells immunolabeled for CD49f identifies 3 division types: (a) symmetric stem cell self-renewal, (b) asymmetric division and (c) symmetric committed cell division. (B): In label-retaining cells, the frequency of asymmetric cell division is far greater than that for symmetric division (96.9% *vs* 3.1% respectively). BrdU$^+$ labeled paired-cell images as indicated. (C): BrdU$^+$ stem cells show a KRT14$^-$/E-cadherin$^-$/WNT10B$^+$ signature. (a-b) BrdU$^+$ and KRT14 labeling during asymmetric division in a paired-cell assay (a) or as whole spheroid (b) show BrdU$^+$ stem cells as KRT14$^-$ and progenitors as KRT14$^+$. (c) BrdU$^+$ cells were E-cadherin negative while progenitor cells are E-cadherin$^+$. (d) BrdU$^+$ cells exhibit high WNT10B immunostain while progenitors are negative. (D-F): CFSE^{Hi} cells exhibit an isolated pattern from neighboring CFSE^{Lo} cells (D, arrows; F) and show larger nuclear diameter and area (E). For diameter and area, CFSE^{Hi} n = 5 and 10, respectively, CFSE^{Lo} n = 108 and 222, respectively. *P < 0.01 *vs* CFSE^{Lo} cells. (F): Confocal image of PS immunostained for Phalloidin/F-actin (red), CFSE$^+$ (green) and DAPI (blue) counterstain. (G): Dual immunolabeling of PS for BrdU$^+$ (red) and LC3 (green) in a paired-cell assay (a) and whole PS (b) reveals increased autophagosome formation in BrdU$^+$ cells. (H): Autophagy flux is specifically activated in BrdU$^+$ labeled stem cells. Far-red, mCherry and GFP were visualized by fluorescent confocal microscopy. The Far-red$^+$ label-retaining cell exhibited high LC3-mCherry stain (purple) but no LC3-GFP fluorescence (arrowhead), indicating fusion of autophagosomes with lysosomes and active autophagy flux in stem cells specifically. Scale bars = 50 μm. See S-Fig. 1 for additional images.

stem cell homeostasis (Clevers et al., 2014), we propose that WNT10B may provide this necessary function in the prostate stem cell niche. Selective expression of *KRT13* and *PRAC1* was also documented in prostate stem cells relative to progenitors and knockdown experiments confirmed their critical role in maintaining stemness properties. A recent study similarly identified KRT13 as enriched in human fetal prostate epithelial cells and confirmed it as a marker for the stem/progenitor population in adult prostate tissue (Liu et al., 2016). Of note, KRT13 plays a directive role in prostate cancer metastasis and its expression in primary prostate tumors is predictive of metastasis and lower survival (Li et al., 2016). Little is known about *PRAC1*, which encodes a small nuclear protein in human prostate and bladder cancer with prognostic capability (Kim et al., 2015; Lenka et al., 2013). That *KRT13* and *PRAC1* are high in normal prostate stem cells and re-expressed in prostate cancers supports the emerging concept that during cancer progression, epithelia transition to a stem-like state that permits their robust growth potential. Together, these stem cell proteins as well as other identified differentially expressed genes may be useful markers in future studies to distinguish stem cells within human prostate tissues.

Data generated from GSEA, DAVID and gene hierarchical clustering of sorted stem and committed progenitor cell transcriptomes provides an opportunity to explore processes that govern prostate stem cell biology, self-renewal and differentiation. One notable enrichment in active stem cells relative to their committed progenitors was genes involved in ribosomal biogenesis and translation initiating factors. Ribosome gene enrichment was similarly observed within the basal cell fraction that contains stem cell markers relative to luminal cells of human benign prostate specimens (Zhang et al., 2016). Recent studies have demonstrated that ribosome biogenesis and translation output levels are critical for stem cell homeostasis and self-renewal while down-regulation of

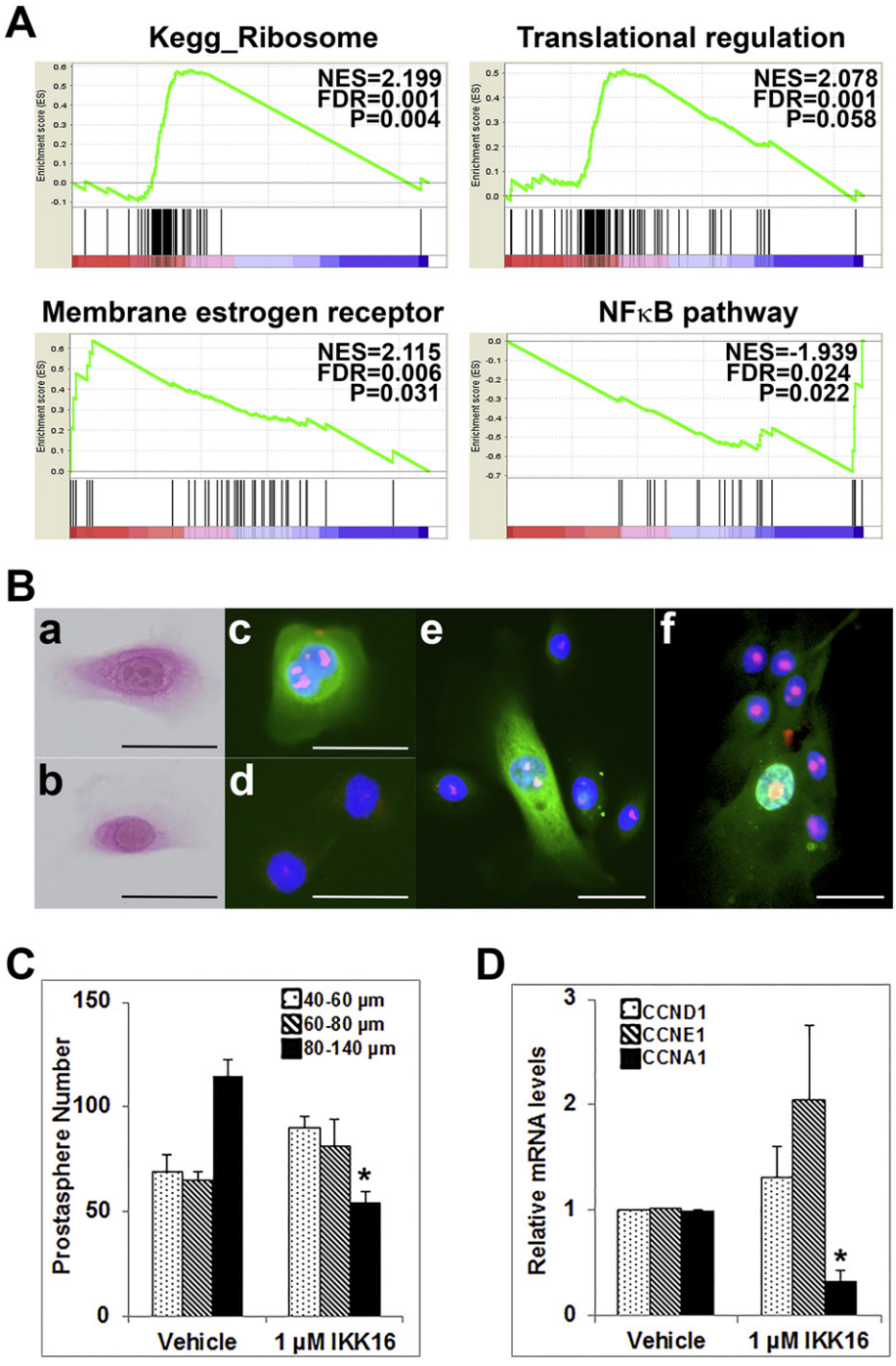

Fig. 4. Next generation RNA-seq followed by Gene Set Enrichment Analysis (GSEA) and biologic confirmation assays reveal enrichment of ribosome, translation regulation and membrane estrogen receptor pathways in $CFSE^{Hi}$ cells while NFκB signaling is enriched in $CFSE^{Lo}$ cells. (A) Next generation RNA-seq data of $CFSE^{Hi}$ and $CFSE^{Lo}$ PS cells (N = 3 biologic replicates) were interrogated by GSEA to identify enriched biologic pathways in stem and daughter progenitor cells, respectively. Significant GSEA Enrichment Score curves (FDR q value < 0.05; FWER P < 0.05) were noted for ribosome and translational regulation (>90% common genes for each), membrane estrogen receptor signaling pathway and the NF-κB pathway. In GSEA thumbnails, the green curve represents the enrichment score curve. Genes on the far left (red) correlated with $CFSE^{Hi}$ cells, and genes on the far right (blue) correlated with $CFSE^{Lo}$ cells. The vertical black lines indicate the position of each gene in the studied gene set. The normalized enrichment score (NES), false discover rate (FDR) and nominal P value are shown for each pathway. (B) Enlarged nucleoli with increased nucleolin protein in $CFSE^{Hi}$ cells. a–d: $CFSE^{Hi}$ (a,c) and $CFSE^{Lo}$ (b,d) cells collected by FACS were H&E stained (a,b) or immune- labeled for Nucleolin protein (pink) with CFSE (green) (c,d). Prominent nucleoli in $CFSE^{Hi}$ stem cells are the site of enhanced ribosome biogenesis in these stem cells. e,f: $CFSE^{Hi}$ (green, e) or $BrdU^{+}$ (green, f) labeled cells were co-immunostained for Nucleolin protein (red) in intact PS, confirming larger nucleoli the label-retaining stem cells relative to progenitors. DAPI nuclear counter stain (blue). Scale bars = 50 μm. (C) Effects of IκB kinase inhibitor IKK16 on day 7 PS number and size. IKK16 decreased the number of larger PS (80–140 μm), indicating reduced proliferation of progenitor cells. *P < 0.001 *vs* Vehicle, N = 3. (D) Cyclin gene expression (CCND1, CCNE1, CCNA1) using qRT-PCR in vehicle and IKK16-treated spheres. NF-κB signaling inhibition significantly decreased CCNA1 mRNA level, indicating cell cycle blockade. *P < 0.001 *vs* Vehicle, N = 3.

rDNA transcription triggers differentiation (Brombin et al., 2015; Zhang et al., 2014). Enlarged nucleoli in $BrdU^{+}/CFSE^{Hi}$ cells with elevated levels of nucleolin, a nucleolar phosphoprotein involved in ribosome synthesis and maturation, provide biologic evidence of enhanced ribosome formation in prostate stem cells. Increased nucleolin further supports the stemness nature of $CFSE^{Hi}$ cells in light of new findings of

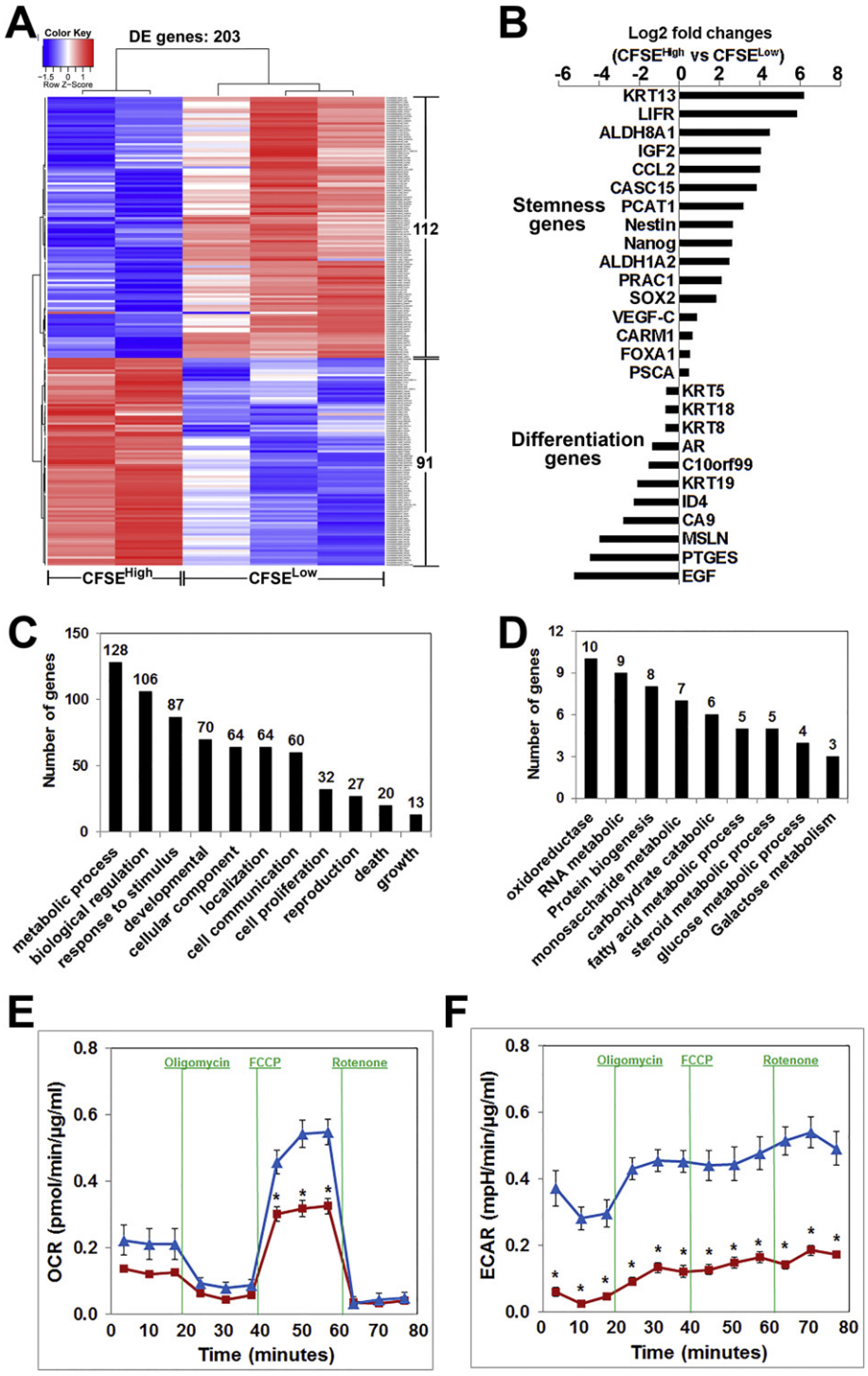

Fig. 5. Gene ontology analysis demonstrate a stemness gene signature and down-regulation of metabolic signaling in CFSE^{Hi} cells, confirmed by metabolic functional assays. (A): Heatmap of 203 significant differentially expressed genes (FDR <0.10) in CFSE^{Hi} (91 enriched genes) *vs* CFSE^{Lo} cells (112 enriched genes) from day 5 PS. (B): Histogram with Log2 fold changes in CFSE^{Hi} *vs* CFSE^{Lo} cells shows enrichment of 16 stem cell genes in CFSE^{Hi} cells and enrichment of 11 known differentiation-associated genes in CFSE^{Lo} cells. (C): Functional annotation using DAVID for the 203 differentially expressed genes revealed enrichment for 11 biological processes in CFSE^{Hi} cells. Numbers above each histogram bar represent the enriched gene numbers. (D): The highest enriched function in CFSE^{Hi} cells, metabolic process, contained 112 down-regulated genes which are further subcategorized for specific pathways. (E-F): Mitochondrial respiratory activity was measured in CFSE^{Hi} and CFSE^{Lo} PS cells by the Seahorse Mito-Stress assay. Oligomysin inhibits ATP synthase (complex V), FCCP uncouples oxygen consumption from ATP production and rotenone inhibits complex I. Relative to the CFSE^{Lo} progenitor cells (blue), CFSE^{Hi} stem cells (red) had decreased levels of basal and maximal oxygen consumption rates (OCR) (E) and lower basal extracellular acidification rates (ECAR) (F). n = 3; * P < 0.05 in E, *P < 0.01 in F *vs* CFSE^{Lo} progenitor cells.

nucleolin's essential role in maintenance of stem cell homeostasis through p53 suppression which enhances nanog expression (Cinghu et al., 2014). While not directly tested herein, elevated expression of both nucleolin and nanog in the CFSE^{Hi} cells suggests a similar regulatory mechanism may exist in the prostate stem cells. Together, these findings implicate CFSE^{Hi} cells as "active" stem cells whereas CFSE^{Lo} cells with reduced ribosome genes are likely committed progenitor cells poised for differentiation.

Autophagy is a major mechanism by which cells survive under stress conditions and stem cells use the same process for life-long survival

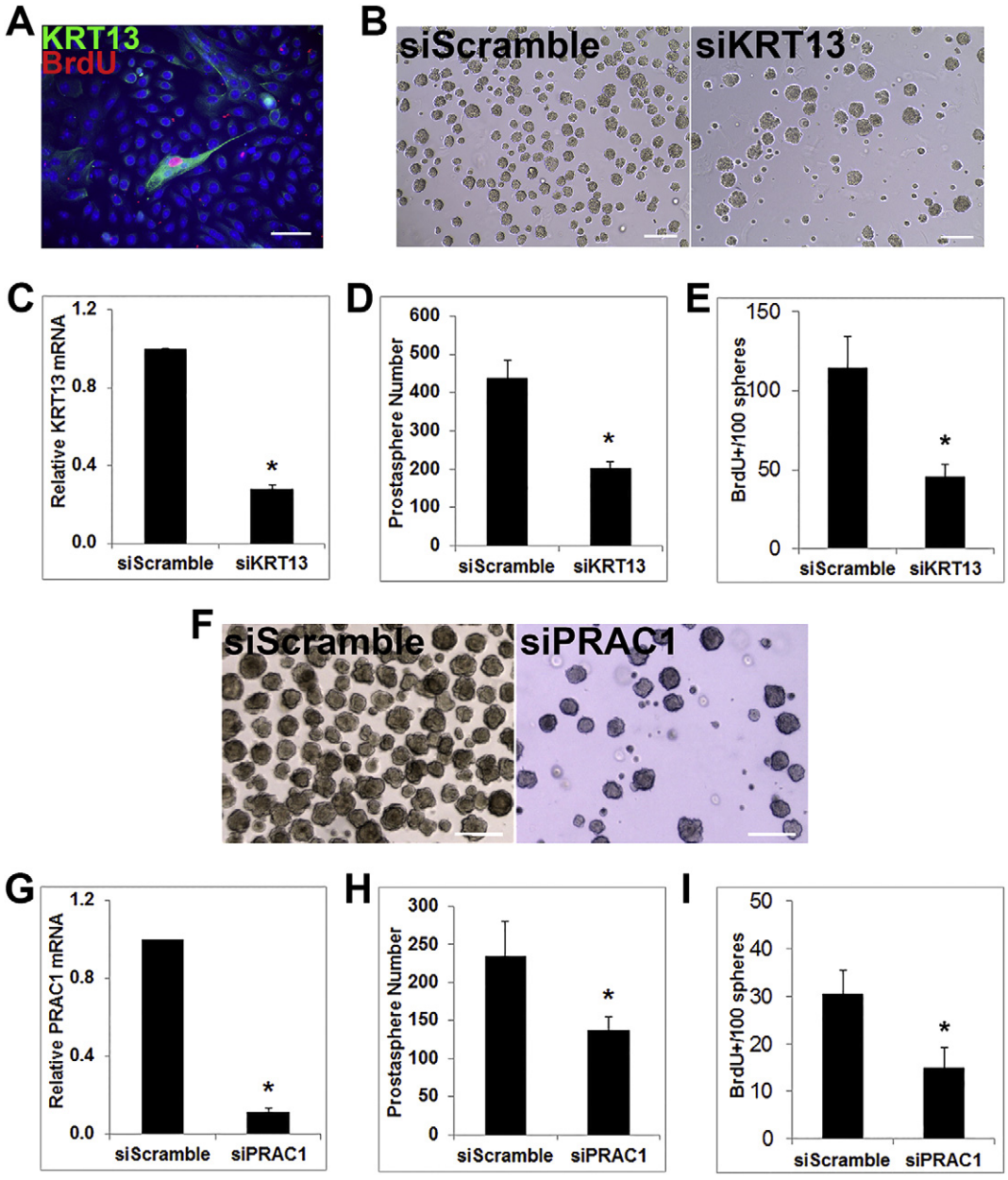

Fig. 6. KRT13 and PRAC1 play essential roles in prostate stem cell maintenance and self-renewal. (A): The $BrdU^+$ stem cell in a day 5 PS shows specific, intense immunostain for KRT13 protein while progenitor cells are negative. Gene knockdown of KRT13 (B-C) or PRAC1 (F-G) in PrEC cells prior to 3D spheroid culture significantly reduced PS numbers (KRT13 B,D; PRAC1 F,H) and the number of $BrdU^+$ label-retaining cells/100 spheres (KRT13 E; PRAC1 I). *$P < 0.05$ *vs* siScramble vector, n = 3 for KRT13, n = 5 for PRAC1. Scale bars = 50 μm.

(Guan et al., 2013; Maycotte et al., 2015). The increased autophagy flux activity in PS label-retaining stem cells relative to the committed progenitors adds to their stem-like characteristics uncovered herein. Remarkably, the present results revealed that during asymmetric division of long-term $BrdU^+$ cells, there is asymmetric DNA inheritance with the daughter progenitor cell receiving newly synthesized DNA while the stem cell retains the parental DNA which supports the immortal stand hypothesis for the human prostate stem cell (Cairns, 1975). Asymmetric segregation of DNA strands appears to occur in stem cells of some, but not all systems (Neumuller and Knoblich, 2009) and may be related to cell turnover rates in different organs. It is considered a mechanism for preserving DNA integrity within the long-lived stem populations and the present data indicate that the prostate stem cell utilizes this cell preservation process.

Anabolic metabolism plays a critical role in dictating whether a cell remains quiescent or proliferates and differentiates and metabolic down-regulation is a distinctive stem cell feature (Ito and Suda, 2014). The present findings of reduced metabolic pathway gene expression with lower mitochondrial oxidative respiration and basal glycolysis supports a relative quiescent stage of prostate stem cells. A recent study showed asymmetric apportioning of mitochondria between stem and progenitor cells following asymmetric division of human mammary stem cells (Katajisto et al., 2015) and it will be of interest to determine whether a similar process contributes to differential metabolic activity in prostate stem cells.

5. Conclusion

The present work has identified unique characteristics of the normal human prostate stem cell population, providing potential markers for future studies and uncovering useful processes that maintain stem cell homeostasis in the prostate gland. The methods derived herein have broad utility in isolating stem cells and more thoroughly characterizing

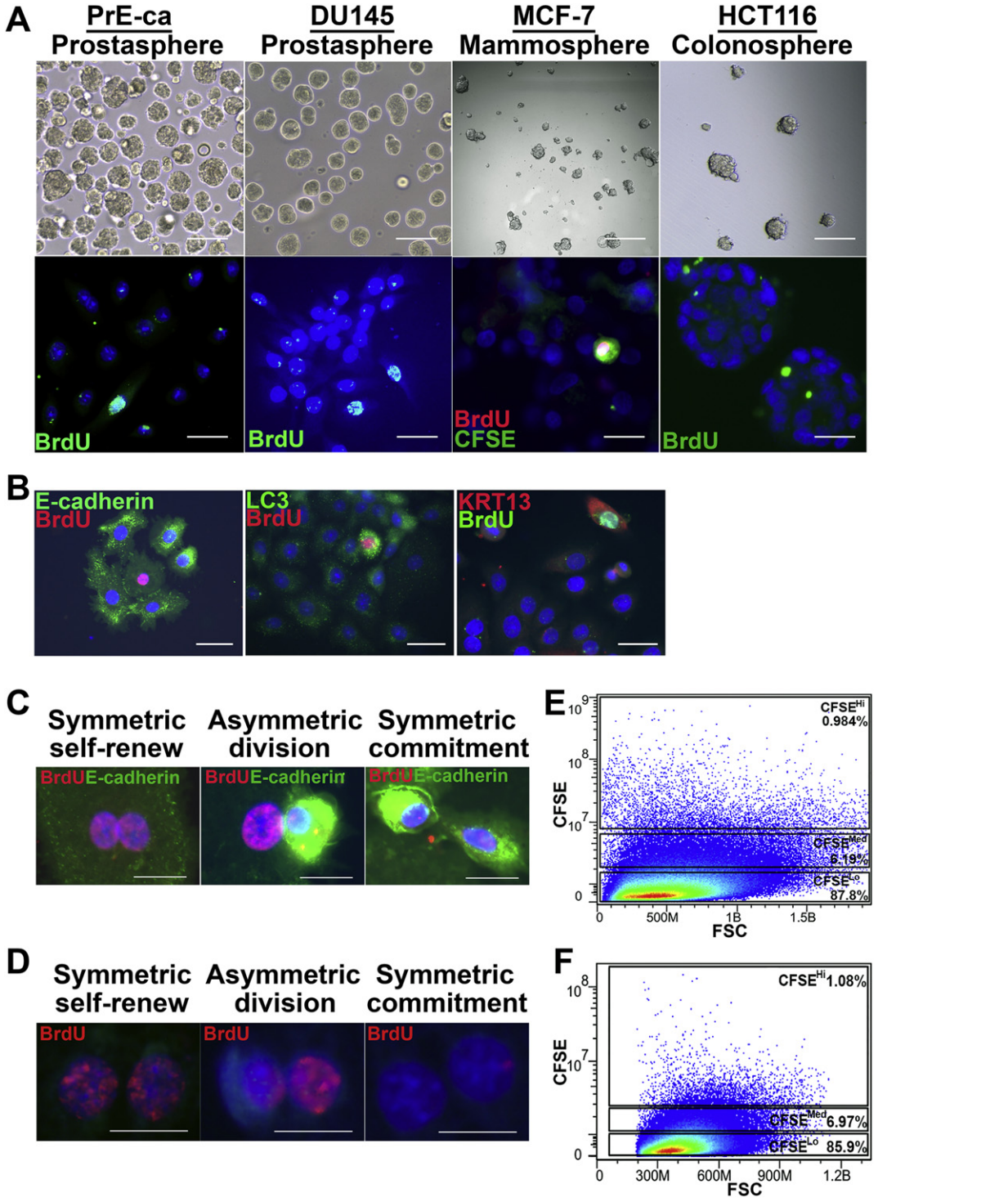

Fig. 7. Sphere-based label-retaining assay identifies cancer stem-like cells. (A): Primary prostate cancer cells (PrE-Ca) and cancer cell lines DU145 (prostate), MCF-7 (breast) and HCT116 (colon) were BrdU/CFSE labeled and cultured in Matrigel to form spheroids. At 1 week, 1–2 $BrdU^+/CFSE^+$ label-retaining cells/sphere were identified, representing the initiating stem-like cell. (B) $BrdU^+$ cancer stem-like cells in PS derived from PrE-Ca exhibited reduced E-cadherin and elevated LC3 and KRT13 protein relative to the non-labeled progenitor cells. (C-D): PrE-Ca (C) and DU145 cells (D) were BrdU-labeled, 3D cultured to PS and dispersed for paired-cell assay with $BrdU^+$ immunolabeling. Stem cell symmetric self-renewal and asymmetric division and progenitor cell symmetric committed divisions were identified in the cancer-derived PSs. (E-F): CFSE-labeled PS derived from PrE-Ca (E) and DU145 (F) cells were dispersed to single cells and live $CFSE^{Hi}$, $CFSE^{Med}$ and $CFSE^{Lo}$ cells were collected by FACS. Scale bars = 50 μm.

their properties, not only from other tissue types but also from cancer specimens which may aid in the discovery of novel therapeutic targets.

Supplementary data to this article can be found online at http://dx.doi.org/10.1016/j.scr.2017.06.009.

Accession numbers

The accession number for the RNA sequencing data reported in this paper is GEO: GSE95542

Acknowledgements

This study was supported by grants from the National Cancer Institute R01-CA172220 (GSP, WYH, LN), R01-ES02207 (GSP, WYH), R01-CA166588, (LN, GSP), and the Michael Reese Research and Education Foundation (GSP, WYH, TS). The authors wish to thank the services of the University of Illinois/Chicago (UIC) Biorepository, Dr. Mark Maienschein-Cline for assistance with bioinformatics analysis, Dr. Alan M. Diamond for providing HCT116 cells, Dr. Marcelo G. Bonini for assistance with Seahorse mito-stress assay, Dr. Susan Kasper, Dr. Hung-Ming Lam and Lynn Birch for assistance in the editing of the manuscript.

References

Allgeier, S.H., Lin, T.M., Moore, R.W., Vezina, C.M., Abler, L.L., Peterson, R.E., 2010. Androgenic regulation of ventral epithelial bud number and pattern in mouse urogenital sinus. Dev. Dyn. 239, 373–385.

Birnie, R., Bryce, S.D., Roome, C., Dussupt, V., Droop, A., Lang, S.H., Berry, P.A., Hyde, C.F., Lewis, J.L., Stower, M.J., et al., 2008. Gene expression profiling of human prostate cancer stem cells reveals a pro-inflammatory phenotype and the importance of extracellular matrix interactions. Genome Biol. 9, R83.

Blackwood, J.K., Williamson, S.C., Greaves, L.C., Wilson, L., Rigas, A.C., Sandher, R., Pickard, R.S., Robson, C.N., Turnbull, D.M., Taylor, R.W., et al., 2011. In situ lineage tracking of human prostatic epithelial stem cell fate reveals a common clonal origin for basal and luminal cells. J. Pathol. 225, 181–188.

Brombin, A., Joly, J.S., Jamen, F., 2015. New tricks for an old dog: ribosome biogenesis contributes to stem cell homeostasis. Curr. Opin. Genet. Dev. 34, 61–70.

Bryant, D.M., Stow, J.L., 2004. The ins and outs of E-cadherin trafficking. Trends Cell Biol. 14, 427–434.

Cairns, J., 1975. Mutation selection and the natural history of cancer. Nature 255, 197–200.

Calderon-Gierszal, E.L., Prins, G.S., 2015. Directed differentiation of human embryonic stem cells into prostate organoids in vitro and its perturbation by low-dose bisphenol a exposure. PLoS One 10, e0133238.

Chen, Z., Palmer, T.D., 2013. Differential roles of TNFR1 and TNFR2 signaling in adult hippocampal neurogenesis. Brain Behav. Immun. 30, 45–53.

Chen, X., Li, Q., Liu, X., Liu, C., Liu, R., Rycaj, K., Zhang, D., Liu, B., Jeter, C., Calhoun-Davis, T., et al., 2016. Defining a population of stem-like human prostate cancer cells that can generate and propagate castration-resistant prostate cancer. Clin. Cancer Res. 22, 4505–4516.

Cicalese, A., Bonizzi, G., Pasi, C.E., Faretta, M., Ronzoni, S., Giulini, B., Brisken, C., Minucci, S., Di Fiore, P.P., Pelicci, P.G., 2009. The tumor suppressor p53 regulates polarity of self-renewing divisions in mammary stem cells. Cell 138, 1083–1095.

Cinghu, S., Yellaboina, S., Freudenberg, J.M., Ghosh, S., Zheng, X., Oldfield, A.J., Lackford, B.L., Zaykin, D.V., Hu, G., Jothi, R., 2014. Integrative framework for identification of key cell identity genes uncovers determinants of ES cell identity and homeostasis. Proc. Natl. Acad. Sci. U. S. A. 111, E1581–E1590.

Clevers, H., Loh, K.M., Nusse, R., 2014. Stem cell signaling. An integral program for tissue renewal and regeneration: Wnt signaling and stem cell control. Science 346, 1248012.

Collins, A.T., Berry, P.A., Hyde, C., Stower, M.J., Maitland, N.J., 2005. Prospective identification of tumorigenic prostate cancer stem cells. Cancer Res. 65, 10946–10951.

Gaisa, N.T., Graham, T.A., McDonald, S.A., Poulsom, R., Heidenreich, A., Jakse, G., Knuechel, R., Wright, N.A., 2011. Clonal architecture of human prostatic epithelium in benign and malignant conditions. J. Pathol. 225, 172–180.

Goldstein, A.S., Lawson, D.A., Cheng, D., Sun, W., Garraway, I.P., Witte, O.N., 2008. Trop2 identifies a subpopulation of murine and human prostate basal cells with stem cell characteristics. PNAS 105, 20882–20887.

Graff, J., Herman, J., Lapidus, R., Chopra, H., Xu, R., Jarrard, D., Isaacs, W., Pitha, P., Davidson, N., Baylin, S., 1995. E-cadherin expression is silenced by DNA hypermethylation in human breast and prostate carcinomas. Cancer Res. 55, 5195–5199.

Guan, J.L., Simon, A.K., Prescott, M., Menendez, J.A., Liu, F., Wang, F., Wang, C., Wolvetang, E., Vazquez-Martin, A., Zhang, J., 2013. Autophagy in stem cells. Autophagy 9, 830–849.

Hu, W.Y., Shi, G.B., Lam, H.M., Hu, D.P., Ho, S.M., Madueke, I.C., Kajdacsy-Balla, A., Prins, G.S., 2011. Estrogen-initiated transformation of prostate epithelium derived from normal human prostate stem-progenitor cells. Endocrinology 152, 2150–2163.

Ito, K., Suda, T., 2014. Metabolic requirements for the maintenance of self-renewing stem cells. Nat. Rev. Mol. Cell Biol. 15, 243–256.

Karthaus, W.R., Iaquinta, P.J., Drost, J., Gracanin, A., van Boxtel, R., Wongvipat, J., Dowling, C.M., Gao, D., Begthel, H., Sachs, N., et al., 2014. Identification of multipotent luminal progenitor cells in human prostate organoid cultures. Cell 159, 163–175.

Katajisto, P., Dohla, J., Chaffer, C.L., Pentinmikko, N., Marjanovic, N., Iqbal, S., Zoncu, R., Chen, W., Weinberg, R.A., Sabatini, D.M., 2015. Stem cells. Asymmetric apportioning of aged mitochondria between daughter cells is required for stemness. Science 348, 340–343.

Kim, Y.W., Yoon, H.Y., Seo, S.P., Lee, S.K., Kang, H.W., Kim, W.T., Bang, H.J., Ryu, D.H., Yun, S.J., Lee, S.C., et al., 2015. Clinical implications and prognostic values of prostate cancer susceptibility candidate methylation in primary Nonmuscle invasive bladder cancer. Dis. Markers 2015, 402963.

Klein, A.M., Simons, B.D., 2011. Universal patterns of stem cell fate in cycling adult tissues. Development 138, 3103–3111.

Lenka, G., Weng, W.H., Chuang, C.K., Ng, K.F., Pang, S.T., 2013. Aberrant expression of the PRAC gene in prostate cancer. Int. J. Oncol. 43, 1960–1966.

Leong, K.G., Wang, B.E., Johnson, L., Gao, W.Q., 2008. Generation of a prostate from a single cell. Nature 456, 804–808.

Li, Q., Yin, L., Jones, L.W., Chu, G.C., Wu, J.B., Huang, J.M., Li, Q., You, S., Kim, J., Lu, Y.T., et al., 2016. Keratin 13 expression reprograms bone and brain metastases of human prostate cancer cells. Oncotarget 7, 84645–84657.

Liu, S., Cadaneanu, R.M., Zhang, B., Huo, L., Lai, K., Li, X., Galet, C., Grogan, T.R., Elashoff, D., Freedland, S.J., et al., 2016. Keratin 13 is enriched in prostate tubule-initiating cells and may identify primary prostate tumors that metastasize to the bone. PLoS One 11, e0163232.

Maycotte, P., Jones, K.L., Goodall, M.L., Thorburn, J., Thorburn, A., 2015. Autophagy supports breast cancer stem cell maintenance by regulating IL6 secretion. Mol. Cancer Res. 13, 651–658.

Miyamoto, D.T., Zheng, Y., Wittner, B.S., Lee, R.J., Zhu, H., Broderick, K.T., Desai, R., Fox, D.B., Brannigan, B.W., Trautwein, J., et al., 2015. RNA-Seq of single prostate CTCs implicates noncanonical Wnt signaling in antiandrogen resistance. Science 349, 1351–1356.

Neumuller, R.A., Knoblich, J.A., 2009. Dividing cellular asymmetry: asymmetric cell division and its implications for stem cells and cancer. Genes Dev. 23, 2675–2699.

Ousset, M., Van Keymeulen, A., Bouvencourt, G., Sharma, N., Achouri, Y., Simons, B.D., Blanpain, C., 2012. Multipotent and unipotent progenitors contribute to prostate postnatal development. Nat. Cell Biol. 14, 1131–1138.

Prins, G.S., Hu, W.Y., Shi, G.B., Hu, D.P., Majumdar, S., Li, G., Huang, K., Nelles, J.L., Ho, S.M., Walker, C.L., et al., 2014. Bisphenol A promotes human prostate stem-progenitor cell self-renewal and increases in vivo carcinogenesis in human prostate epithelium. Endocrinology 155, 805–817.

Prins, G.S., Calderon-Gierszal, E.L., Hu, W.Y., 2015. Stem cells as hormone targets that lead to increased cancer susceptibility. Endocrinology 156, 3451–3457.

Smith, B.A., Sokolov, A., Uzunangelov, V., Baertsch, R., Newton, Y., Graim, K., Mathis, C., Cheng, D., Stuart, J.M., Witte, O.N., 2015. A basal stem cell signature identifies aggressive prostate cancer phenotypes. Proc. Natl. Acad. Sci. U. S. A. 112, E6544–E6552.

Toivanen, R., Mohan, A., Shen, M.M., 2016. Basal progenitors contribute to repair of the prostate epithelium following induced luminal anoikis. Stem Cell Rep. 6, 660–667.

Vander Griend, D.J., Karthaus, W.L., Dalrymple, S., Meeker, A., DeMarzo, A.M., Isaacs, J.T., 2008. The role of CD133 in normal human prostate stem cells and malignant cancer-initiating cells. Cancer Res. 68, 9703–9711.

Wang, Z.A., Mitrofanova, A., Bergren, S.K., Abate-Shen, C., Cardiff, R.D., Califano, A., Shen, M.M., 2013. Lineage analysis of basal epithelial cells reveals their unexpected plasticity and supports a cell-of-origin model for prostate cancer heterogeneity. Nat. Cell Biol. 15, 274–283.

Wang, J., Zhu, H.H., Chu, M., Liu, Y., Zhang, C., Liu, G., Yang, X., Yang, R., Gao, W.Q., 2014. Symmetrical and asymmetrical division analysis provides evidence for a hierarchy of prostate epithelial cell lineages. Nat. Commun. 5, 4758.

Wang, B.E., Wang, X., Long, J.E., Eastham-Anderson, J., Firestein, R., Junttila, M.R., 2015. Castration-resistant Lgr5(+) cells are long-lived stem cells required for prostatic regeneration. Stem Cell Reports 4, 768–779.

Williamson, S.C., Mitter, R., Hepburn, A.C., Wilson, L., Mantilla, A., Leung, H.Y., Robson, C.N., Heer, R., 2013. Characterisations of human prostate stem cells reveal deficiency in class I UGT enzymes as a novel mechanism for castration-resistant prostate cancer. Br. J. Cancer 109, 950–956.

Xin, L., Lukacs, R.U., Lawson, D.A., Cheng, D., Witte, O.N., 2007. Self-renewal and multilineage differentiation in vitro from murine prostate stem cells. Stem Cells 25, 2760–2769.

Yun, E.J., Zhou, J., Lin, C.J., Hernandez, E., Fazli, L., Gleave, M., Hsieh, J.T., 2016. Targeting cancer stem cells in castration-resistant prostate cancer. Clin. Cancer Res. 22, 670–679.

Zhang, Q., Shalaby, N.A., Buszczak, M., 2014. Changes in rRNA transcription influence proliferation and cell fate within a stem cell lineage. Science 343, 298–301.

Zhang, D., Park, D., Zhong, Y., Lu, Y., Rycaj, K., Gong, S., Chen, X., Liu, X., Chao, H.P., Whitney, P., et al., 2016. Stem cell and neurogenic gene-expression profiles link prostate basal cells to aggressive prostate cancer. Nat. Commun. 7, 10798.